

RESEARCH

Open Access



Efficient production of itaconic acid from the single-carbon substrate methanol with engineered *Komagataella phaffii*

Manja Mølgaard Severinsen¹, Simone Bachleitner¹, Viola Modenese^{1,3}, Özge Ata^{1,2} and Diethard Mattanovich^{1,2*}

Abstract

Background Amidst the escalating carbon dioxide levels resulting from fossil fuel consumption, there is a pressing need for sustainable, bio-based alternatives to underpin future global economies. Single-carbon feedstocks, derived from CO₂, represent promising substrates for biotechnological applications. Especially, methanol is gaining prominence for bio-production of commodity chemicals.

Results In this study, we show the potential of *Komagataella phaffii* as a production platform for itaconic acid using methanol as the carbon source. Successful integration of heterologous genes from *Aspergillus terreus* (*cadA*, *mttA* and *mfsA*) alongside fine-tuning of the *mfsA* gene expression, led to promising initial itaconic acid titers of 28 g·L⁻¹ after 5 days of fed-batch cultivation. Through the combined efforts of process optimization and strain engineering strategies, we further boosted the itaconic acid production reaching titers of 55 g·L⁻¹ after less than 5 days of methanol feed, while increasing the product yield on methanol from 0.06 g·g⁻¹ to 0.24 g·g⁻¹.

Conclusion Our results highlight the potential of *K. phaffii* as a methanol-based platform organism for sustainable biochemical production.

Introduction

Due to the continuous exploitation of fossil fuels, the atmospheric content of carbon dioxide is rapidly increasing [1], and it becomes clear that alternative, sustainable, bio-based products and feedstocks must form the foundation of the global economy in the future. Efforts are underway to pioneer novel technologies and production platforms for products traditionally produced from gas, coal or oil [2, 3]. Many of these advancements use

microbial systems to enable conversion of organic materials into biofuels as well as chemicals with a wide range of complexity [4–8]. The replacement of fossil resources with renewable first-generation feedstocks, however, raises social and ethical concerns due to the high demand for alternative food and feed sources driven by the growing world population [9, 10]. Naturally, this has prompted greater technological investment in alternative substrates, aiming for a neutral carbon footprint and sidestepping ethical implications. Sustainable resources of interest include various waste products such as crude glycerol [11], lignocellulosic biomass [12], food waste [13] and more unconventionally single-carbon (C1) substrates derived from CO₂ [14]. Valorising CO₂ and its derived C1 substrates is a growing area of interest, being developed in various biotechnological [4, 15–17] and chemical fields [18]. Methanol (MeOH), a low-cost renewable

*Correspondence:

Diethard Mattanovich
diethard.mattanovich@boku.ac.at

¹ Department of Biotechnology, Institute of Microbiology and Microbial Biotechnology, BOKU University, 1190 Vienna, Austria

² Austrian Centre of Industrial Biotechnology, 1190 Vienna, Austria

³ Department of Food, Environmental and Nutritional Sciences, University of Milan, Milan, Italy



© The Author(s) 2024. **Open Access** This article is licensed under a Creative Commons Attribution 4.0 International License, which permits use, sharing, adaptation, distribution and reproduction in any medium or format, as long as you give appropriate credit to the original author(s) and the source, provide a link to the Creative Commons licence, and indicate if changes were made. The images or other third party material in this article are included in the article's Creative Commons licence, unless indicated otherwise in a credit line to the material. If material is not included in the article's Creative Commons licence and your intended use is not permitted by statutory regulation or exceeds the permitted use, you will need to obtain permission directly from the copyright holder. To view a copy of this licence, visit <http://creativecommons.org/licenses/by/4.0/>. The Creative Commons Public Domain Dedication waiver (<http://creativecommons.org/publicdomain/zero/1.0/>) applies to the data made available in this article, unless otherwise stated in a credit line to the data.

single-carbon feedstock, is gaining attention for bio-production of commodity chemicals. With the additional interest in MeOH, production capacity has increased to 174 million metric tons by 2022 and is steadily increasing [19]. Traditionally sourced from syngas, MeOH can now also be generated from methane and CO₂, offering a means of sequestering greenhouse gasses to support a sustainable bio-economy [20]. Methylophilic organisms, possessing the inherent capability to utilize MeOH as their exclusive carbon and energy source, stand out as promising candidates as platform organisms, with the yeast *Komagataella phaffii* being one of them [20–22]. Although *K. phaffii* is widely recognized in the industry for recombinant protein production [23], recent findings indicate its significant potential in generating platform chemicals [24–27].

One platform chemical gaining an increasing worldwide interest is itaconic acid (IA), an unsaturated dicarboxylic acid, which holds considerable promise as a biochemical building block, as its versatility lies in its ability to serve as a monomer for various products such as resins, plastics, paints, and synthetic fibers [28, 29]. Traditionally, microbial production of IA started in 1960 by fermenting *Aspergillus terreus* in sugar-containing media [30]. Other microorganisms such as *Ustilago* sp., *Candida* sp. and *Rhodotorula* sp. have since shown the ability to produce IA; however, *A. terreus* has remained the predominant industrial production host, achieving titers of up to 150 g·L⁻¹ during a cultivation for 9.7 days [13, 31–33]. The natural biosynthetic pathway for IA follows a pathway analogous to citric acid formation, involving the tricarboxylic acid cycle (TCA). In *A. terreus*, IA is produced from *cis*-aconitate by the key enzyme aconitate decarboxylase, *CadA*, residing in the cytosol [34–36]. Further two transporters are involved in shuttling either the precursor *cis*-aconitate from the mitochondria to the cytosol, i.e., the mitochondrial *cis*-aconitate transporter (*MttA*) or the product itself to the extracellular space, i.e., the major facilitator superfamily transporter (*MfsA*) [36, 37]. The commercial production of IA by *A. terreus* has improved since its establishment [31, 38, 39], but it mainly relies on monosaccharides that could also be utilized as food or feed. Alternative, more sustainable substrates for production with *A. terreus* or alternative hosts have long been under investigation, with MeOH being one of the least explored [30, 38, 40, 41]. Production using the C1-substrate could potentially lower manufacturing costs, contribute to a circular economy and improve the overall production sustainability [15, 16, 20]. Hence, *K. phaffii* as a natural methylotroph and established production host in biotechnology is a promising candidate for producing itaconic acid from MeOH.

In this study, we explored the potential of *K. phaffii* as a production organism for IA using MeOH as the primary carbon source. For that, the heterologous genes *cadA*, *mttA* as well as *mfsA* from *A. terreus* were successfully engineered into *K. phaffii*. The engineered pathway is illustrated in Fig. 1. Upon small-scale preliminary experiments in 24-deep-well plates and shake flasks, fed-batch cultivations were carried out in lab-scale reactors, where optimal results were achieved by combining strain engineering with process engineering.

Methods

Cloning and yeast transformation

The *Komagataella phaffii* wild-type strain CBS7435 (Centraalbureau voor Schimmelcultures, NL) was used as a host for engineering the initial itaconic acid (IA) producing strain, the *cadA* strain. In CBS7435, a single copy of the *cis*-aconitate decarboxylase gene from *A. terreus*, *cadA* (ATEG_09971) was genomically integrated under the control of the *pAOX1* in the *RGI2* locus using CRISPR-Cas9. In a similar manner, the *cadA*+*mttA* strain was generated, where both transcription units, *cadA* and *mttA* (ATEG_09970), were incorporated into the *RGI2* locus in CBS7435. For *mttA* expression, the *pPOR1* promoter was used. For the *cadA*+*mttA*+*mfsA* strains, homologous recombination of the *mfsA* gene (ATEG_09972) encoding a cytoplasmic IA exporter was inserted into the *GUT1* locus by CRISPR-Cas9 in the *cadA*+*mttA* strain. To find the optimal expression strength of *mfsA*, different promoters (*pGAP*, *pFDH1*, *pPOR1*, *pFBA1*) were tested. The *cadA*+*mttA*+*mfsA*_{*pGAP*} strain was used as host for generation of the multicopy strains (MC). To allow random

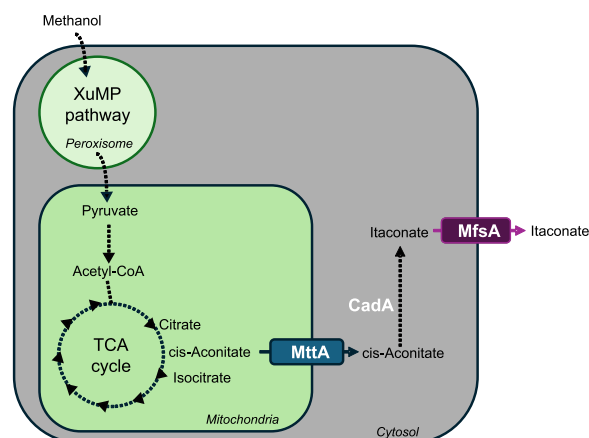


Fig. 1 The engineered metabolic pathway for itaconic acid production from methanol in *K. phaffii*. *CadA*: *cis*-aconitate decarboxylase, *MttA*: mitochondrial *cis*-aconitate transporter, *MfsA*: Major Facilitator Superfamily transporter of itaconic acid

integration of heterologous genes via non-homologous end joining, plasmids of the respective genes were created with unspecific homologous overhangs and without the assistance of CRISPR-Cas9. dDNA was prepared by linearization using *AscI* and PCR purification (Jena Bioscience PP-201L). Transformations were facilitated in a single round to generate strains with multiple copies of the individual genes; of *cadA* and *mfsA*; and of all three genes simultaneously. The transformed multicopy clones were plated and selected on plates with high zeocin concentrations (300, 600, 1000 $\mu\text{g}\cdot\text{mL}^{-1}$). Integrations of donor DNA (dDNA) into correct loci or random integration were verified via PCR for all clones. A list of the strains used in this study are listed in Table 1.

The dDNA, consisting of the respective heterologous genes flanked by the homologous sequences of the respective integration loci, was prepared by PCR amplification using Q5[®] high-fidelity DNA polymerase from the respective plasmids.

Primers and plasmids were designed using Qiagen CLC genomics workbench. Primers were ordered at Eurofins Genomics, sequences and names can be found in Table S1. All plasmids were designed using the Golden Gate Assembly (GGA) and the CRISPR-Cas9 systems developed and described by Prielhofer et al. and Gassler et al. [42, 43], utilizing *Escherichia coli* DH10B as host. *E. coli* were transformed with the respective plasmids via heat-shock, transformants were then grown on LB plates with either 50 $\mu\text{g}\cdot\text{mL}^{-1}$ kanamycin or 50 $\text{mg}\cdot\text{mL}^{-1}$ ampicillin [42, 43].

Transformation of *K. phaffii* was performed as described by Gasser et al. [44]. To summarize, 80 μL of competent *K. phaffii* cells was gently mixed with the linearized DNA and the CRISPR-Cas9 vector [42, 43], the mixture was then transferred to a chilled electroporation cuvette for 5 min, and electroporated with BioRad Gene Pulser[™] for 4 ms (2000 V, 25 μF , 200 Ω). The transformed

cells were then mixed with cold YPD and regenerated for 2 h at 28 °C before plating on YPD or YPG plates with respective antibiotics (kanamycin or zeocin) and incubation at 30 °C for 2 days.

24-deep-well plate screenings

First screenings to identify producing strains were performed in 24-deep-well plates of 2 mL cultures for 48 h. Here, a two-phase screening protocol was used, as described by Gasser et al. [44]. The first phase consisted of biomass production, where selected clones were cultivated in 2 mL YPG precultures overnight at 25 °C or 30 °C and 280 rpm. The main cultures were initiated by inoculating buffered yeast nitrogen base (YNB; 3.4 $\text{g}\cdot\text{L}^{-1}$, pH 5.5–6.0, supplemented with 10 $\text{g}\cdot\text{L}^{-1}$ $(\text{NH}_4)_2\text{SO}_4$ as the nitrogen source, 10 mM potassium phosphate buffer) to a starting OD_{600} of 4. The cells were induced with 0.5% MeOH (v/v) and incubated at 25 °C or 30 °C and 280 rpm. For the following 48 h, the cells were fed twice per day with 2% MeOH (v/v). Samples for monitoring of cell growth (OD_{600}) and metabolite concentrations were taken at the end of the cultivation and the best-producing clones were identified and selected for further screening based on the calculated $Y_{\text{P/X}}$.

Shake flask cultivations

A screening of generated strains was performed in small-scale shake flask cultivations. As in the 24-deep-well plate screenings, a two-phase system was used [44]. For biomass production, strains were inoculated in a 10 mL YPG preculture (yeast extract 10 $\text{g}\cdot\text{L}^{-1}$, soy peptone 20 $\text{g}\cdot\text{L}^{-1}$, glycerol 20 $\text{g}\cdot\text{L}^{-1}$) overnight at 30 °C and 180 rpm. Cells from the preculture were subsequently used for inoculation of the main culture with a starting OD_{600} of 4. For that, the cells were cultivated in 250 mL wide neck flasks, with a starting volume of 25 mL buffered YNB, at 30 °C and 180 rpm. Cells were

Table 1 *K. phaffii* strains used in this study

Short name	Genotype	References
<i>K. phaffii</i> WT	CBS7435	[45]
cadA	pAOX1_cadA	This study
cadA + mttA	pAOX1_cadA + pPOR1_mttA	This study
cadA + mttA + mfsA _{pGAP}	pAOX1_cadA + pPOR1_mttA + pGAP_mfsA	This study
cadA + mttA + mfsA _{pFDH1}	pAOX1_cadA + pPOR1_mttA + pFDH1_mfsA	This study
cadA + mttA + mfsA _{pPOR1}	pAOX1_cadA + pPOR1_mttA + pPOR1_mfsA	This study
cadA + mttA + mfsA _{pFBA1}	pAOX1_cadA + pPOR1_mttA + pFBA1_mfsA	This study
MC I	5.9 × pAOX1_cadA + 2.0 × pPOR1_mttA + 2.6 × pGAP_mfsA	This study
MC II	5.2 × pAOX1_cadA + 1.6 × pPOR1_mttA + 3.7 × pGAP_mfsA	This study
MC III	4.3 × pAOX1_cadA + 4.0 × pPOR1_mttA + 1.0 × pGAP_mfsA	This study

induced with 0.5% MeOH (v/v) and fed twice a day with 2% MeOH (v/v) for approximately 70 h. Cell growth (OD_{600}) was monitored throughout the cultivation and extracellular metabolite concentrations (MeOH, IA) were quantified by high-performance liquid chromatography (HPLC), as described below.

To investigate the tolerance to itaconic acid, a toxicity screening was performed in shake flasks as described above with minor changes; YNB medium was supplemented with IA to reach final concentrations of 25 g·L⁻¹, 50 g·L⁻¹, and 100 g·L⁻¹ respectively, pH was adjusted to 5.5 with KOH. Throughout the toxicity screening, pH was measured and viability investigated via PI staining as described below.

Fed-batch cultivation

Fed-batch cultivations were carried out in a DAS-GIP parallel bioreactor system (Eppendorf bioreactors SR0700ODLS and SR1000ODLS). To prepare the bioreactor inoculum, 100 mL YPG in a 1000 mL shake flask was inoculated with 1 mL of a working cell bank from the respective strain and incubated at 25 °C, 180 rpm overnight (~16 h). Three hours before batch inoculation, 50 mL YPG was added to each shake flask. Cells equivalent to reach a batch OD_{600} of 1 were used to inoculate the batch medium, modified BSM medium (13.5 mL·L⁻¹ H₃PO₄ (85%), 0.5 g·L⁻¹ CaCl₂·2H₂O, 7.5 g·L⁻¹ MgSO₄·7H₂O, 9 g·L⁻¹ K₂SO₄, 2 g·L⁻¹ KOH, 46.51 g·L⁻¹ glycerol, 4.4 g·L⁻¹ citric acid monohydrate, 0.25 g·L⁻¹ NaCl, 8.70 mL·L⁻¹ Biotin (0.1 g·L⁻¹), 0.1 mL·L⁻¹ Glanapon2000, 19.14 mL·L⁻¹ 25% NH₃, 4.35 mL·L⁻¹ PTM0 (6.00 g·L⁻¹ CuSO₄·5H₂O, 0.08 g·L⁻¹ NaI, 3.36 g·L⁻¹ MnSO₄·H₂O, 0.20 g·L⁻¹ Na₂MoO₄·2H₂O, 0.02 g·L⁻¹ H₃BO₃, 0.82 g·L⁻¹ CoCl₂, 20.00 g·L⁻¹ ZnCl₂, 65.00 g·L⁻¹ FeSO₄·7H₂O, 5 mL·L⁻¹ H₂SO₄ (95–98%)). Dissolved oxygen concentration was controlled at 30% by adjusting the stirrer speed, inlet gas flow and O₂ concentration, where 200 rpm, 9.5 sL·h⁻¹ and 21% were the minimal setpoints, and 1250 rpm, 50 sL·h⁻¹ and 100% were the maximum setpoints.

In the preliminary fermentation, the batch phase was followed by an 8 h phase of glycerol-medium feed (550 g·L⁻¹ 99% glycerol, 10.4 mL·L⁻¹ PTM0, 10.4 mL·L⁻¹ Biotin (0.2 g·L⁻¹)) at a rate of 0.225·t + 1.95, again followed by a co-feed phase of 17.5 h where the glycerol-medium feed rate decreased over time (3.65–0.111·t mL·h⁻¹) as the MeOH feed increased (0.028·t + 0.6 mL·h⁻¹). After the co-feed phase, the MeOH feed was continued at the same rate for the remaining time of the fermentation. The pH was maintained at 5.5 using 25% NH₃ to counteract the acidification caused by the cultivation.

Modification of fed-batch cultivations

To prevent continuous biomass accumulation in the remaining fermentations, the base used for pH control was changed to 5 M KOH, and the feeding strategy was altered. The glycerol concentration of the modified mBSM was decreased to 33 g·L⁻¹ to allow 20 g·L⁻¹ of biomass at the end of the batch phases. The batch phases of ~20 h were followed by 4 h of a limited glycerol-feed phase (500 mL·L⁻¹ glycerol), with no additional trace elements or biotin. The limited glycerol-feed phase was performed to reach a biomass of ~40 g·L⁻¹ and to induce the MeOH-inducible genes [46]. A limited MeOH feed was then applied for the rest of the cultivation. The MeOH feed was adapted throughout the respective fermentation to prevent MeOH depletion as well as toxification.

Sampling and production analysis of fed-batch cultivations

For all fed-batch cultivations, samples were taken with time intervals for analysis of OD_{600} , microscopy, dry cell weight (DCW) and HPLC, furthermore viability and samples for RNA extraction were included in some fermentations. For the respective fermentations, the bioreactor model, starting volume of the batch phase, final volume, glycerol-medium-feed rate and MeOH-feed rate are noted with the final biomass and IA titers are noted in Table S2. Specific growth rates and production parameters were calculated according to the equations listed in Table 2.

HPLC measurements

A Biorad Aminex HPX-87H HPLC column (300×7.8 mm) was used for the HPLC measurements. H₂SO₄ at a concentration of 4 mM was used as mobile phase, with a 0.6 mL·min⁻¹ flow rate at 60 °C. IA was measured with a photodiode array detector (SPD-M20A, Shimadzu) at 254 nm. MeOH and glycerol concentrations

Table 2 Equations used to calculate production parameters

Parameter	Equation
μ [h ⁻¹]	$\frac{\ln(\frac{X_2}{X_1})}{t_2 - t_1}$
q_p [g·g ⁻¹ ·h ⁻¹]	$\frac{P_2 - P_1}{(X_1 + 0.67 \cdot (X_2 - X_1)) \cdot (t_2 - t_1)}$
q_s [g·g ⁻¹ ·h ⁻¹]	$\frac{S_2 - S_1}{(X_1 + 0.67 \cdot (X_2 - X_1)) \cdot (t_2 - t_1)}$
Space Time Yield (STY) [g·L ⁻¹ ·h ⁻¹]	$\frac{P_2 - P_1}{(t_2 - t_1) \cdot V}$
$Y_{p/S}$ [g·g ⁻¹]	$\frac{P_2 - P_1}{S_2 - S_1}$
$Y_{p/X}$ [g·g ⁻¹]	$\frac{P_2 - P_1}{(X_1 + 0.67 \cdot (X_2 - X_1))}$
$Y_{X/S}$ [g·g ⁻¹]	$\frac{X_2 - X_1}{S_2 - S_1}$

X: viable biomass [g] based on yeast dry mass (YDM) measurements, t: time [h], P: total itaconic acid [g], S: total methanol consumed [g], V: volume [L]. For estimation of q_p , q_s and $Y_{p/X}$, the biomass responsible for the IA production between two sampling points was estimated with a two-point moving average

were quantified with a refraction index detector (RID-10A, Shimadzu). The chromatograms obtained with both detectors were used to confirm the absence of by-products in relevant concentrations. Prior to HPLC measurement, samples were vortexed and centrifuged at full speed (16,100 g) for 5 min at room temperature. After centrifugation, the supernatant of each sample was mixed with H₂SO₄ (40 mM) resulting in a final concentration of 4 mM. The supernatants were then filtered through a 0.22 µm filter into vials for the HPLC analysis.

PI staining

To measure the viability of fed-batch yeast cultures, samples were diluted in PBS (0.24 g·L⁻¹ KH₂PO₄, 1.8 g·L⁻¹ Na₂HPO₄·2 H₂O, 0.2 g·L⁻¹ KCl, 8.0 g·L⁻¹ NaCl) to an OD₆₀₀ of 0.1–0.4 and stained with a propidium iodide (PI) stock solution to final concentrations of 2.0 M. PI acts as a DNA-intercalating fluorescent dye that permeates cells with compromised cell membranes thereby indicating cell death. When PI binds to DNA, it leads to a strong increase in red fluorescence (excitation/emission at 480/630 nm) [47]. Samples were analyzed on a CytoFlex S Flow Analyser 4L 13 (Color, Beckman Coulter), where the percentage of viable cells was estimated based on PI negativity.

RNA extraction and subsequent cDNA conversion

Throughout the fermentations, cell pellets were harvested and quenched with 1 mL TRI Reagent (SigmaAldrich) and frozen until further processing. RNA from 25 mg of yeast cell mass per 1 mL TRI reagent was extracted by lysing the cells with ~500 µL glass-beads at 5.5 m/s for 2–40 s. Samples were then incubated at RT for 5 min before addition of 200 µL chloroform and vortexing for 15 s and incubation for 10 min at RT. To separate the RNA from DNA and protein, a centrifugation step was performed (4 °C, 10 min, 10,000 g) and the aqueous phase was mixed with 500 µL 2-propanol and incubated at RT for 8 min. The RNA was then pelleted by an additional centrifugation step (4 °C, 10 min, 10,000g) and subsequently washed with 70% ethanol. When all ethanol had evaporated, the RNA was solubilized with 80 µL water (65 °C, 12 min). Residual genomic DNA was degraded with the DNA-free™-kit (Invitrogen) following the suppliers' protocol.

The quality, purity and concentration of the isolated RNA was analyzed with Nanodrop and visual analysis of an SYBR Safe agarose gel, and the absence of gDNA was verified by a PCR with primers homologous to the gene, *ACT1* and subsequent gel electrophoresis. cDNA synthesis was performed with the Biozym cDNA Synthesis Kit in accordance with the manufacturer's protocol, using oligo d(T)23 VN (NEB) primers.

Extraction of genomic DNA (gDNA)

Genomic DNA of the respective *K. phaffii* strains was extracted from overnight cultures using the Wizard Genomic DNA purification kit (Promega Corp., USA) according to the manufacturer's instructions. The quality, purity and concentration of the isolated gDNA was analyzed with Nanodrop.

Analysis of relative gene copy numbers and gene expression

RT-qPCR was performed by mixing 2×qPCR S'Green BlueMix (Biozym Blue S'Green qPCR Kit), cDNA, water and qPCR primers (Table S1) in accordance with the supplier's instructions. All samples were tested in technical duplicates and negative controls, without cDNA, were included for all primers. The quantitative gene expression analysis was performed using a real-time PCR cyclor (Rotor Gene, Qiagen) and subsequent data analysis using the comparative quantitation (QC) method of the Rotor Gene software.

The GCNs of the *K. phaffii* multicopy strains (MC) were estimated by comparing the relative quantification of the interest sequences of the heterologous genes to that of the parent strain, *cadA* + *mttA* + *mfsA*_{pGAP}, in which a single copy of the respective heterologous genes had been inserted locus-specifically via homologous recombination guided by CRISPR-Cas9. The GCNs were subsequently estimated relative to the corresponding parent strain using the threshold cycle ($\Delta\Delta CT$) method [48].

The differences in gene expression among strains in different bioreactors were estimated by comparing the relative quantification of the respective reactor to the reference bioreactor at the same sampling time point. All signals were normalized to the constitutively expressed reference gene *ACT1* (PP7435_Ch3-0993).

Results

Enabling itaconic acid production from methanol in *K. phaffii*

Due to the absence of genes encoding a *cis*-aconitate decarboxylase, naturally occurring strains of *K. phaffii* are incapable of producing itaconic acid (IA). A recent study [49] has shown that a synthetic autotrophic *K. phaffii* could be engineered to produce IA from CO₂ by insertion of a single gene, *cadA* from the natural producer *A. terreus*. The IA production was further improved by the insertion of another *A. terreus* gene encoding the mitochondrial *cis*-aconitate transporter, *mttA*.

In this study, a wild-type *K. phaffii* CBS7435 strain was engineered to produce IA from methanol (MeOH) by the integration of three heterologous genes from *A. terreus* in the *K. phaffii* genome. Initially, *cadA* encoding

for the key enzyme was placed under the control of the strong MeOH-inducible alcohol oxidase 1 promoter (*pAOX1*) [42, 50] resulting in the *cadA* strain. Next, *mttA* was inserted under the regulation of a moderately strong constitutive promoter (*pPOR1*) [42], referred to hereafter as the *cadA + mttA* strain. Lastly, the *A. terreus* gene *mfsA*, encoding for a cytoplasmic membrane transporter specific to IA export, was integrated generating the *cadA + mttA + mfsA* strains. Previous studies have shown that modulating the transporter activity in vivo is crucial for optimal cell metabolism and productivity [49, 51]. For that reason, different promoters (*pFDHI*, *pGAP*, *pPOR1*, *pFBA1* [42, 50]) were tested for the expression of *mfsA*, in the *cadA + mttA* strain background. A 24-deep-well plate screening was performed to evaluate the IA production of the newly generated *cadA + mttA + mfsA* strains, and the IA yield, $Y_{P/X}$, is given in Fig. 2a. Notably, a strong promoter regulation of *mfsA* was beneficial for producing IA yielding comparable results obtained with the strong constitutive *pGAP* and the MeOH-inducible *pFDHI* promoter. The best-producing *cadA + mttA + mfsA_{pGAP}* clone was selected arbitrarily for further experiments, based on the screening results, and the benefits of having a constitutive expression of the product exporter.

To gain a comprehensive overview of how the expression of various genes of the IA pathway impacts IA production, we cultivated the strains *cadA*, *cadA + mttA*, and *cadA + mttA + mfsA_{pGAP}* along with the CBS7435 strain as a reference in a comparative shake flask screening (Fig. 2b), where samples for HPLC, pH measurements and viability (Figure S1) were taken at time intervals. While expression of *cadA* alone yielded 0.23 g·L⁻¹ after 70 h, additional expression of *mttA* improved the IA titers eightfold to 1.8 g·L⁻¹. Additional expression of *mfsA* further boosted the production with an additional 65% reaching 3.0 g·L⁻¹ after 70 h (Fig. 2b). Intriguingly, growth was not affected by the expression of *cadA*, whereas additional expression of *mttA* reduced growth by 47% and whereas additional expression of *mfsA* restored the growth to 75% of the *cadA* strain.

Itaconic acid production from methanol in fed-batch cultivations is feasible

To investigate whether the high IA productivity of the *cadA + mttA + mfsA_{pGAP}* strain was transferable to a larger scale, a fed-batch cultivation was performed with *cadA + mttA + mfsA_{pGAP}* alongside the *cadA + mttA* strain as a reference. The initial bioreactor setup for IA production was inspired by the setup for protein production of *K. phaffii* [52], since this was the standard for *K. phaffii* bioprocesses and as organic acid production from MeOH at that time had not been established in our laboratory. Therefore, a standard four-phase protocol

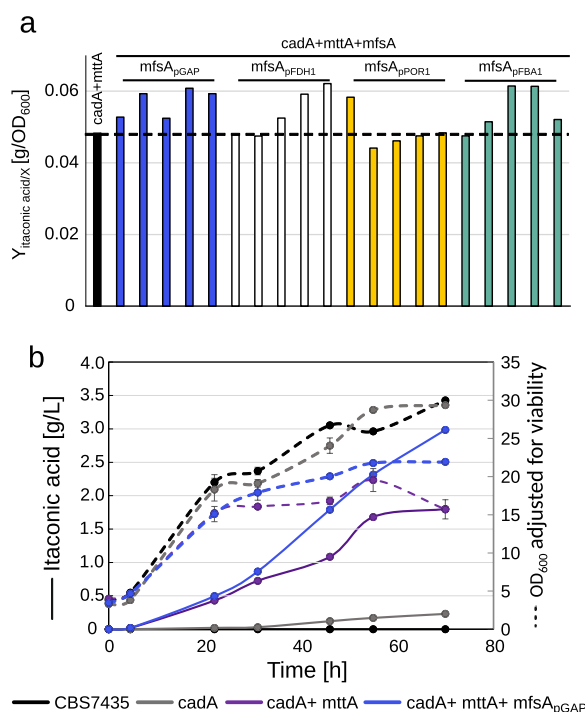


Fig. 2 Fine-tuning promoter balance of the MfsA transporter is beneficial for itaconic acid production. **a** Itaconic acid yields of the *cadA + mttA* strain compared to five clones of each *cadA + mttA + mfsA* strain after 48 h of cultivation at 25 °C for choice of best promoter for *mfsA* expression, **b** comparative shake flask cultivation of the CBS7435, *cadA*, *cadA + mttA*, *cadA + mttA + mfsA_{pGAP}* strains performed at 30 °C. Throughout the cultivation, samples were taken for OD₆₀₀, HPLC and pH measurements, and for investigation of the viability of the strains with PI staining. The OD₆₀₀ is adjusted to exclude unviable cells. All strains were cultivated in duplicates, and average values and standard deviations for growth and itaconic acid production are shown

was used, consisting of an initial glycerol batch phase for biomass production reaching 32 g·L⁻¹ of biomass after 27 h, a 8 h glycerol-medium feed phase followed by a 17-h-long co-feed phase for a gradual MeOH gene activation [46], and finally a pure MeOH-feed phase for organic acid production. During the MeOH-feed phase the biomass increased from 85 g·L⁻¹ to 140 g·L⁻¹. The dissolved oxygen concentration (DO) was controlled at 30% and pH was maintained at 5.5 by an automatic addition of 25% NH₃. In Fig. 3, the IA and growth profiles of the fermentation are shown.

The 20% increase in production observed in the shake flask screening (Fig. 2b) was reproducible on a larger scale, reaching 22.9 and 28.2 g·L⁻¹ of IA by *cadA + mttA* and *cadA + mttA + mfsA_{pGAP}* respectively, resulting in an overall increase of 22% by the additional expression of *mfsA* (Fig. 3) and a 40% increase in the yield on MeOH (Table 3). However, despite these improvements, the average yield per gram of MeOH remained at 0.1 g·g⁻¹,

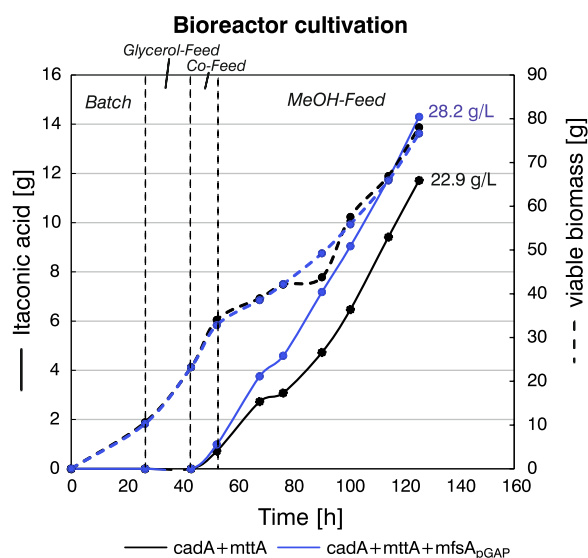


Fig. 3 Upscaling of *cadA* + *mttA* + *mfsA_{pGAP}* cultivation leads to high itaconic acid production. Growth and production profiles are shown for the *cadA* + *mttA* and *cadA* + *mttA* + *mfsA_{pGAP}* strains. To ensure comparability of results despite varying cultivation volumes resulting from continuous MeOH and base feed, total amounts rather than concentrations are presented. The final IA titers [$\text{g}\cdot\text{L}^{-1}$] are also shown. Time axis corresponds to the whole cultivation time including all four phases, i.e., batch, glycerol feed, co-feed and MeOH feed

primarily due to significant biomass accumulation (Table 3 and Table S2). This continuous biomass accumulation was expected given the fermentation strategy, which was originally developed for protein production

favoring high cell densities. The continuous growth was enabled by a nutrient-rich complex medium (modified mBSM) and an ongoing nitrogen replenishment through the addition of NH_3 as a base control.

Increasing fermentation temperature doubles itaconic acid yields in nitrogen limitation

To further optimize the IA production of the *cadA* + *mttA* + *mfsA_{pGAP}* strain, the following adjustments of the fermentation process were applied. First, to prevent high biomass formation as observed in the previous fermentation, a nitrogen limitation was introduced by changing the base from the 25% NH_3 to 5 M KOH. Consequently, only nitrogen present in the batch medium was utilized by the cells for biomass formation. Second, the glycerol-feed and co-feed phases were replaced by a restricted glycerol feed lasting 4 h. These adjustments made the process less time-consuming and resulted in a comparable effective activation of the MeOH-utilizing genes [46]. Finally, as the enzymatic activity of CadA had shown a positive correlation with temperatures up to 42 °C [35], the process temperature was elevated from 25 °C to 30 °C, one of the highest tolerated temperatures for *K. phaffii* [53]. The IA production and growth profiles of the fermentation are shown in Fig. 4. Throughout the fermentation, samples were taken and analyzed as in the previous fed-batch cultivation with additional samples for PI staining to gain a better insight of the cell viability throughout the process (Figure S2a). As a clear trend

Table 3 Average values of key production parameters obtained from the methanol feed phase of the fed-batch cultivations

Strain	Temperature	μ_{VDM} [h^{-1}]	$Y_{\text{P/X}}$ [$\text{g}\cdot\text{g}^{-1}$]	$Y_{\text{P/S}}$ [$\text{g}\cdot\text{g}^{-1}$]	STY [$\text{g}\cdot\text{L}^{-1}\cdot\text{h}^{-1}$]	q_{P} [$\text{g}\cdot\text{g}^{-1}\cdot\text{h}^{-1}$]	q_{S} [$\text{g}\cdot\text{g}^{-1}\cdot\text{h}^{-1}$]	$Y_{\text{X/S}}$ [$\text{g}\cdot\text{g}^{-1}$]	IA [$\text{g}\cdot\text{L}^{-1}$]
<i>cadA</i> + <i>mttA</i>	25 °C	0.01	0.03	0.07	0.18	0.002	0.96	0.44	23.0
<i>cadA</i> + <i>mttA</i> + <i>mfsA_{pGAP}</i>		0.02	0.04	0.10	0.36	0.004	0.95	0.42	28.2
<i>cadA</i> + <i>mttA</i> + <i>mfsA_{pGAP}</i>	25 °C	0.02	0.06	0.05	0.15	0.003	1.60	0.29	6.2
	30 °C	0.02	0.13	0.09	0.32	0.007	1.70	0.25	13.3
<i>cadA</i> + <i>mttA</i> + <i>mfsA_{pGAP}</i>	30 °C	0.01	0.10	0.14	0.25	0.005	0.80	0.18	27.2
MC I		0.01	0.20	0.24	0.45	0.009	0.97	0.17	49.5
MC II		0.01	0.17	0.22	0.40	0.007	0.89	0.20	45.6
MC III		0.01	0.14	0.19	0.31	0.006	0.85	0.11	32.9
MC I	28 °C	0.01	0.20	0.24	0.40	0.009	0.85	0.23	45.3
	30 °C	0.01	0.21	0.26	0.45	0.009	0.88	0.20	49.7
	32 °C	0.01	0.22	0.23	0.49	0.010	1.09	0.14	55.4
	34 °C	0.01	0.21	0.24	0.44	0.009	0.93	0.16	49.1

The productivity parameters are calculated for the methanol feed phases of the respective fermentations, according to the equations in Table 2. Mean specific growth rates (μ_{VDM}), IA yield per gram of viable biomass ($Y_{\text{P/X}}$), IA yield per gram of methanol, the space time yield (STY) indicating the volumetric productivity per hour, the specific IA production rate per gram of viable biomass (q_{P}), specific methanol consumption rate (q_{S}), the average biomass yield per methanol ($Y_{\text{X/S}}$) and the final IA titer. Biomass concentration analyses used for μ_{VDM} and productivity calculations were performed in triplicate. The biomass concentrations for the last three fed-batch cultivations were adjusted for viability based on the results of a propidium iodide staining (Figure S2)

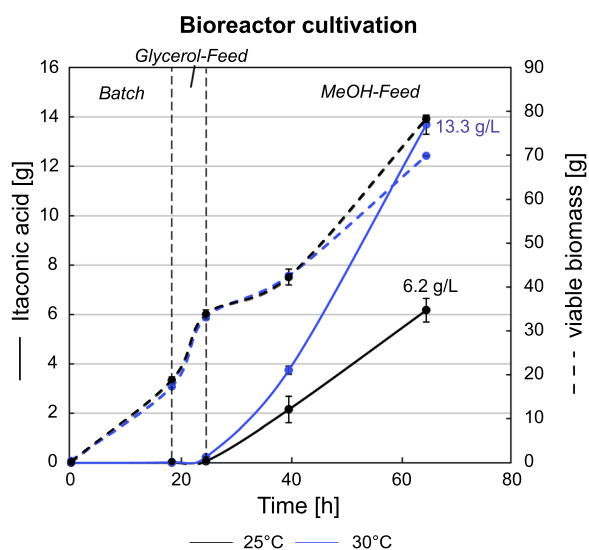


Fig. 4 Temperature dependency of itaconic acid production in *K. phaffii* favors a higher temperature. Growth and production profiles are shown for the *cadA* + *mttA* + *mfsA*_{PGAP} strain cultivated at 25 °C and 30 °C. To ensure comparability of results, total amounts rather than concentrations are presented. The final IA titers [g·L⁻¹] are also shown. The time axis corresponds to the whole cultivation time including all three phases, i.e., batch, glycerol feed and MeOH feed. The growth profile at 30 °C is markedly lower than at 25 °C, which in combination with the improved IA production clarifies that a cultivation temperature of 30 °C is favorable

Intriguingly, the production efficiency increased markedly along with the elevated process temperature. As indicated in Fig. 4 and the calculated production parameters in Table 3, the average yield per biomass was more than doubled (+123%), while the conversion of MeOH into IA was doubled simultaneously with a 13% decrease in the biomass accumulation after only 64 h. In terms of titers, elevation of the process temperature by 5 °C pushed the IA concentrations from 6.2 g·L⁻¹ to 13.3 g·L⁻¹ after only 40 h of MeOH-feed phase, suggesting that a higher process temperature is significantly beneficial for IA production.

Integrating multiple copies of itaconic acid pathway genes improves production when the right balance between genes is achieved

Elevating the gene copy number (GCN) of heterologous biosynthesis genes is a common strategy to enhance productivity of strains. In other synthetic IA producers, it has recently been demonstrated that increasing the GCN of *cadA* improves IA production [54, 55]. Similarly, the push-and-pull effect has previously been shown to promote production of other organic compounds [49, 56, 57]. Hence, we aimed to increase the GCN of *cadA*, *mttA* and *mfsA* either individually or in a combined approach. For that, the *cadA* + *mttA* + *mfsA*_{PGAP} strain was transformed with plasmids for multicopy integration of either *cadA*, *mttA* or *mfsA*, or the following combinations: *cadA* + *mfsA* and *cadA* + *mttA* + *mfsA*. A set of the generated multicopy (MC) clones was cultivated

was already observed after 64 h, the fermentation was stopped and evaluated.

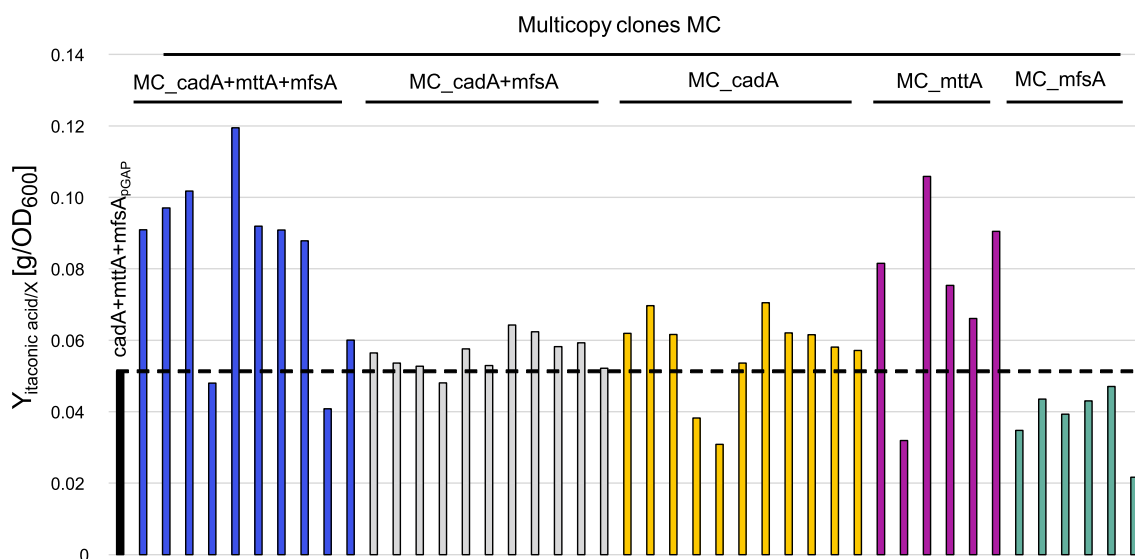


Fig. 5 Integration of multiple copies of the heterologous genes doubles itaconic acid yield. The yield per biomass (OD₆₀₀) was evaluated for the individual multicopy clones and compared with the *cadA* + *mttA* + *mfsA*_{PGAP} parental strain after 48 h of cultivation with a 2% MeOH feed in 24-deep-well plates

in 24-deep-well plates for 48 h (Fig. 5). In addition, all clones were tested for their GCN via a quantitative PCR approach (Figure S3a-c). Based on the OD_{600} and the IA concentration (Table S3), the individual clones were evaluated by calculating the IA yield per biomass (Fig. 5).

Upon analyzing the IA production alongside the gene copy numbers (GCN) of the heterologous genes (Fig. 5 and Figure S3a-c), it is evident that inserting multiple copies of *cadA* or *mfsA* as individual genes, as well as the multicopy combination *cadA+mfsA*, has a limited or even negative effect on IA production in most clones. The majority of the MC_ *cadA+mttA+mfsA* clones showed increased yields, indicating that multicopy integration of all three heterologous genes, *cadA+mttA+mfsA*, is necessary to improve the IA yield, provided that the optimal balance of the three genes is reached. Surprisingly, several of the MC_ *mttA* clones showed a high productivity per biomass, however, the production titers were low, and so the high yields were only enabled by a low biomass accumulation (Figure S3d and Table S3). When analyzing the OD_{600} with the GCN, a correlation between a high GCN of *mttA* with an impaired growth in both the MC_ *mttA* and the MC_ *cadA+mttA+mfsA* clones is observed.

Despite the high $Y_{P/X}$, the strains with a high *mttA* GCN were likely unfit for longer fed-batch cultivations.

Based on the 24-deep-well plate screening (Fig. 5), and subsequent shake flask cultivations (Figure S4), three clones (hereafter referred to MC I, MC II and MC III) were selected for a fed-batch cultivation along with the *cadA+mttA+mfsA*_{pGAP} parent strain. MC I and II were chosen as they had shown the highest IA production alongside parent-like growth, while MC III was selected for its relatively high IA production combined with a decreased growth phenotype (Figure S3). The fed-batch cultivation was performed as the previously described three-phase cultivation at 30 °C. Samples were extracted continuously to allow for analysis of growth, IA production and viability, and furthermore samples for RNA extraction were included.

Going in line with the results from the previous screenings, all MC strains showed improved IA production (Fig. 6a). Specifically, MC I showed the highest IA titers of 49.5 g·L⁻¹, followed by MC II with 45.6 g·L⁻¹ and MC III with 32.9 g·L⁻¹. The parent strain *cadA+mttA+mfsA*_{pGAP} reached only 27.2 g·L⁻¹. MC III exhibited a notable reduction in biomass formation while growth rates remained similar between the parent strain,

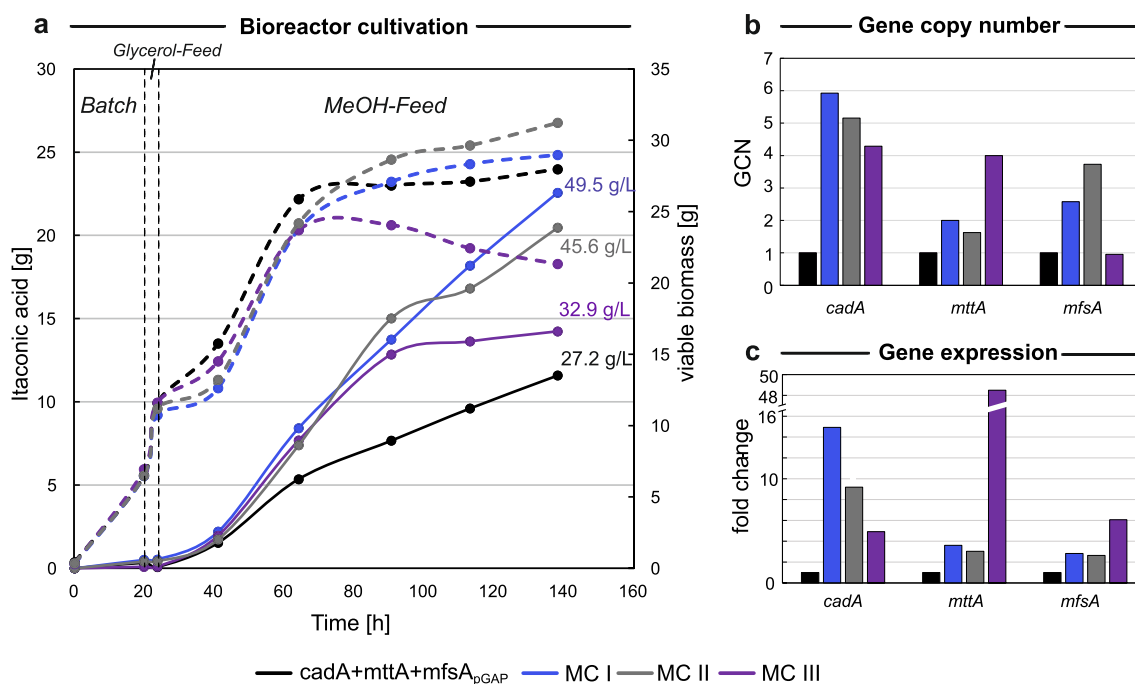


Fig. 6 Balancing the gene copy number of the three heterologous genes enables titers of 49.5 g·L⁻¹ after 5 days of fed-batch cultivation. **a** Growth and production profiles are shown for the *cadA+mttA+mfsA*_{pGAP} strain and three selected multicopy strains (MC I, MC II and MC III) cultivated at 30 °C. To ensure comparability of results, total amounts rather than concentrations are presented, the final IA titers [g·L⁻¹] are also shown. The time axis corresponds to the whole cultivation time including all three phases, i.e., batch, glycerol feed and MeOH feed. All MC strains show an increased IA production compared to the parental strain. **b** Gene copy numbers of the three multicopy strains relative to the parental strain with single copy integration of all three heterologous genes. **c** The relative expression of the three heterologous genes at the fermentation for the three multicopy strains normalized to the expression of the parental strain at the same time point

MC I, and MC II (Fig. 5a). The MC III shows a decline in biomass after 80 h of cultivation, this is in line with the previous experiments and an observed correlation between growth impairments and high *mttA* GCN. The *mttA* GCN of MC III is double that of the other strains (Fig. 6b). High GCN of *cadA* and *mfsA*, in combination with a slight increase in the GCN of *mttA*, is beneficial for IA production, as implicated by MC I and MC II (Fig. 6a, b). To verify if a higher GCN correlates with an elevated expression of the genes, RNA was extracted at different time points throughout the fermentation, and subsequently, cDNA was analyzed via RT-qPCR. As gene expression was found to be highest at the end of fermentation, this particular time point is depicted in Fig. 6c. In alignment with the GCN, expression levels of the heterologous genes *cadA* and *mttA* were elevated accordingly, suggesting a direct correlation between GCN and gene expression and indicating that the multiple copies are active. Interestingly, the trend between GCN and fold change is not observed for *mfsA* expression in all three MC clones. Instead, the MC III, with a high *mttA* GCN and an extremely high *mttA* expression level, shows the highest *mfsA* expression, suggesting that the high *mttA* expression affects the expression of *mfsA*. Overall, with generating multicopy strains the IA production could markedly be improved, resulting in an improvement of the average STY by up to 80% and $Y_{P/S}$ up to 71% when compared to the parental strain under

identical cultivation conditions (Table 3). The production efficiency of MC I was moderately higher than MC II, but when taking the observed viability drop for MC II (Figure S2b) into account, MC I did not only show the highest productivity, it also showed the highest robustness, making it the optimal strain for subsequent experiments.

Expression of *mfsA* improves tolerance to itaconic acid

High IA concentrations both within and outside the cells might burden the cells. Especially with high *mttA* expression, which increases the substrate availability for *CadA*, IA accumulation in the cytosol is probable. High intracellular IA concentrations are likely to have a negative effect on cell metabolism. Strong expression of *mfsA* can, therefore, be beneficial for the well-being of the cell, as it facilitates the export of IA and maintains a low cytosolic pool of the organic acid. To evaluate (i) if the generated strains are suitable for high IA production in general and (ii) if differences exist in IA tolerance between the engineered strains, a toxicity screening was performed. Therefore, the *cadA*, *cadA*+*mttA*, *cadA*+*mttA*+*mfsA*_{pGAP}, and the MC I strain were cultivated alongside the CBS7435 strain in the presence of high external IA concentrations in the range of 25, 50 and 100 g·L⁻¹ at a pH range of 5.5–5.7. OD₆₀₀ and viability were measured throughout the screening and are depicted in Fig. 7.

Interestingly, IA concentrations in the range of 25 g·L⁻¹ inhibited growth of the CBS7435, the *cadA*

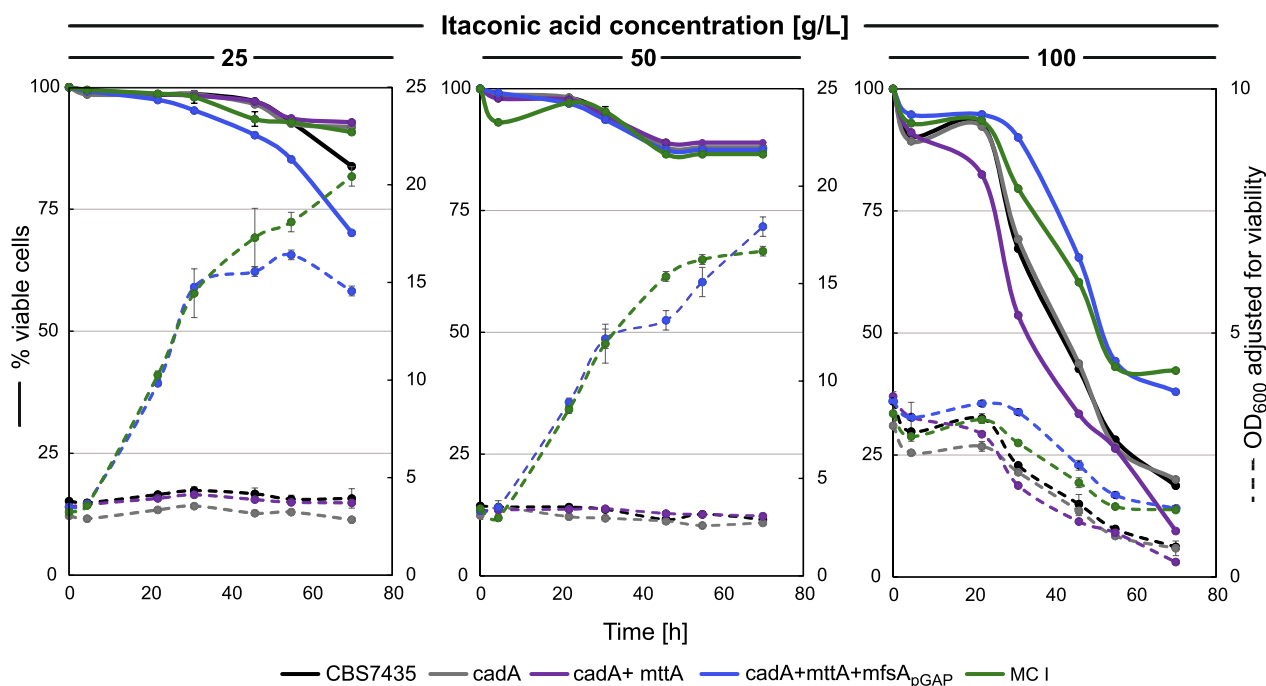


Fig. 7 Expression of *mfsA* improves *K. phaffii*'s tolerance to extracellular itaconic acid. The four engineered strains were cultivated in parallel with CBS7435 in cultivations with high IA concentrations (25, 50 and 100 g·L⁻¹) at 30 °C

strain and *cadA*+*mttA* strain. Under these conditions, only strains expressing the *MfsA* transporter, i.e., *cadA*+*mttA*+*mfsA*_{pGAP} and MC I, demonstrated growth. Similar results were obtained in cultivations with 50 g·L⁻¹ of IA. Throughout these conditions, viability remained relatively stable, not dropping below 70%. However, at IA levels of 100 g·L⁻¹, both the *cadA*+*mttA*+*mfsA*_{pGAP} and MC I strain were adversely affected in the utilized cultivation conditions, as observed in the declining biomass profile (Fig. 7). Nonetheless, both strains exhibited better performance with their viability stabilizing at 38–42% compared to CBS7435, *cadA*, and *cadA*+*mttA* strains where viability dropped below 20%. These results clearly indicate that the expression of *mfsA* improves the tolerance to IA.

Optimal process temperatures are between 30 and 32 °C for the MC I strain in fed-batch bioreactor cultivations

Having successfully engineered a high IA producer strain, MC I, through multicopy gene integration, we proceeded with a final fermentation experiment aimed at optimizing the process temperature. For that, the same three-phase fed-batch strategy was used, testing fermentation temperatures of 28, 30, 32 and 34 °C. Samples were extracted for growth- and HPLC as well as for viability analysis. IA and growth profiles are depicted in Fig. 8. At 28 °C, biomass formation was improved rather than IA production, while 34 °C resulted in a lower biomass and IA profiles. In all cases, strains maintained a high viability throughout the fermentation process (Figure S2c), at 34 °C the viability did, however, drop to 70.5%. The best results were observed within the temperature range of 30–32 °C, resulting in titers between 50 and 55 g·L⁻¹ IA. While 32 °C showed 7–10% higher overall production parameters for production ($Y_{P/X}$, STY, q_P), the MeOH conversion to IA was 10% more favorable at 30 °C (Table 3). Therefore, 30 °C was deemed optimal for a sustainable production of IA from MeOH. Based on the results obtained with the MC I strain cultivated at 30 °C (Figs. 6 and 8), the reproducibility of the production process was confirmed. An overlay of the two performed fed-batch cultivations with MC I at 30 °C is shown in Figure S5.

Discussion

Traditionally, itaconic acid (IA) production has primarily been associated with filamentous fungi such as *Aspergillus spp.* or *Ustilago maydis* using glucose as a carbon source [39, 58, 59]. However, the search for alternative hosts has been ongoing, driven by the need for more sustainable production methods and the exploration of diverse substrates. In this study, we show that *K. phaffii* can produce IA from methanol (MeOH) reaching titers between 50 and 55 g·L⁻¹. This was achieved by a

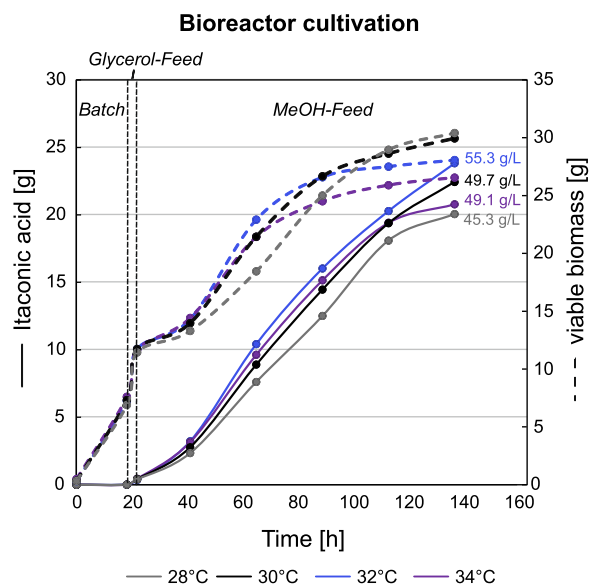


Fig. 8 Fed-batch cultivation of the engineered *K. phaffii* strain shows highest IA production between 30 and 32 °C. Growth and production profiles are shown for the MC I strain at different cultivation temperatures (28, 30, 32, and 34 °C). To ensure comparability of results, total amounts rather than concentrations are presented, together with the final IA titers [g·L⁻¹]. Time axis corresponds to the whole cultivation time including all three phases, i.e., batch, glycerol feed and MeOH feed

combinatorial approach focusing on strain engineering and process optimization.

In several natural non-producing organisms, overexpression of *cadA* has enabled IA production from different carbon substrates, including C1 feed stocks [58]. Just to mention a few, *cadA* expression enabled *Methylorubrum extorquens* AM1 IA production from MeOH reaching titers of 31.6 mg·L⁻¹ [60], and autotrophic IA production from CO₂ was enabled in strains such as *Synechocystis* sp. PCC6803 and a synthetic autotrophic *K. phaffii* strain, yielding 14.5 mg·L⁻¹ and 530 mg·L⁻¹, respectively [49, 61]. Also in our hands, expression of *cadA* enabled IA production in the range of 0.23 g·L⁻¹ on MeOH in *K. phaffii*. The production capacity was, however, boosted with the coexpression of the *MttA* transporter, reaching titers of 1.8 g·L⁻¹. Expression of *mttA* creates possibly a pull effect of *cis*-aconitate from the mitochondria to the cytosol, thereby providing more precursor molecules for conversion by *CadA* to IA [62, 63]. Further, we demonstrated that by incorporating an *A. terreus* gene encoding a plasma membrane transporter, *mfsA*, under the control of a strong promoter, IA titers of 3.0 g·L⁻¹ were reached in shake flask cultivations. The pivotal role of both transporters has previously been underscored by Wierckx et al. [64], a finding corroborated by our observations. Furthermore, our results suggested

that utilizing a strong promoter for *mfsA* proves advantageous for IA production. Subsequent toxicity screenings revealed that MfsA expression also improved growth and viability of *K. phaffii* at high IA concentrations. This phenomenon is likely attributed to the efficient export of IA by the cell, thereby mitigating weak organic acid-induced stress within the cellular environment.

Upscaling the process to bioreactor cultivations was successful, reaching IA titers of $28.2 \text{ g}\cdot\text{L}^{-1}$ with the strain expressing a single copy of all three heterologous genes *cadA*, *mttA* and *mfsA*. However, excessive biomass accumulation was a significant side effect, hence process optimization was required. The combination of nitrogen limitation and an increase in process temperature from 25 to 30 °C resulted in a twofold increase in the MeOH yield for the *cadA*+*mttA*+*mfsA*_{pGAP} strain. In addition, it led to a 13% reduction in biomass accumulation, favoring the conversion of MeOH to IA over biomass production. A substantial increase in IA production was anticipated, considering the prior evaluation of CadA activity [35]. Here, in vitro studies revealed a positive correlation between enzyme activity and temperature, peaking at 42 °C in *A. terreus*. Further process optimization of the multicopy strains, exploring temperatures ranging from 28 to 34 °C, revealed that the engineered strain exhibited optimal performance within the temperature range of 30–32 °C. Notably, cellular metabolism was adversely impacted by 34 °C leading to decreased viability over time and less efficient MeOH utilization compared to a temperature of 30 °C. This decline in cell viability is particularly undesirable for downstream processing of the fermentation broth, as reduced viability results in increased cell lysis and thus presence of unwanted cell debris [65]. The absence of metabolic by-products during all fed-batch cultivations was confirmed with HPLC analysis, which would further simplify downstream isolation of IA.

Next to this, we could show that increasing the number of all heterologous genes markedly improved the potential of *K. phaffii* as an IA production host, as it increased IA productivity ($0.45 \text{ g}\cdot\text{L}^{-1}\cdot\text{h}^{-1}$) simultaneously with an efficient conversion of MeOH into IA ($0.26 \text{ g}\cdot\text{g}^{-1}$). In several organisms [54, 55], the integration of multiple copies of *cadA* has proven beneficial for production. The instability of CadA was previously described [31, 66], though whether the necessity for additional *cadA* expression is linked to this instability remains unanswered at this point. However, our findings suggest that the integration of additional *cadA* copies had a minimal impact on IA production in *K. phaffii*, unless it coincides with the multicopy integration of *mttA* and *mfsA*. The heightened expression of these two transport proteins enhanced

the pull effect. Notably, strains harboring a high *mttA* GCN showed severe growth impairments in comparison to the remaining multicopy strains. Similar results were obtained by Baumschabl et al. [49], indicating that a strong promoter regulation for *mttA* expression severely impacts growth in the autotrophic *K. phaffii* strain. A high MttA activity might efficiently drain the TCA cycle from its intermediate and result in accumulation of IA in the cytosol, thus possibly inflicting acid-induced stress within the cell. The additional expression of *mfsA* in the *cadA*+*mttA*+*mfsA*_{pGAP} and MC_*cadA*+*mttA*+*mfsA* strains possibly compensates for this phenotype as IA-toxication becomes less likely due to the increased export.

Conclusion

Overall, the success of our IA production process using *K. phaffii* as a platform is attributed to the combined efforts of metabolic engineering and process engineering, emphasizing the importance of both aspects in developing efficient and sustainable production processes. Although our strain cannot yet compete with industrially relevant yields of $0.58 \text{ g}\cdot\text{g}_{\text{glucose}}^{-1}$ produced by *A. terreus* [33] in terms of carbon conversion, one must consider the origin of the carbon, as the use of glucose in the current industrial process is unfavorable for a sustainable development of bio-based production. Our process establishes for the first time a high-yield MeOH-based production system with a high IA production rate of $0.45 \text{ g}\cdot\text{L}^{-1}\cdot\text{h}^{-1}$. This high production rate in combination with the advantages of MeOH as carbon source, the additional safety of *K. phaffii* as a non-pathogenic, well-established production host and the minimal by-product formation streamlining downstream purification highlight the relevance of our process. With additional metabolic and process engineering advancements, *K. phaffii* is poised to emerge as a significant industrial production host for IA utilizing MeOH.

Supplementary Information

The online version contains supplementary material available at <https://doi.org/10.1186/s13068-024-02541-1>.

Supplementary Material 1.

Acknowledgements

We want to thank Viktoria Kowarz and Bernhard Schmelzer for their great help in performing some of the fed-batch cultivations. M.M.S. was further supported by the Bioprocess Engineering Doctoral School of BOKU University.

Author contributions

M.M.S., S.B., O.A. and D.M. contributed to the design of the work. M.M.S., V.M. and S.B. were involved in data acquisition. M.M.S., S.B., O.A. and D.M. were involved in data analysis. M.M.S., S.B. and D.M. wrote the manuscript. D.M. acquired funding. All the authors read and approved the final manuscript.

Funding

This work was supported by the project 'Innovative bio-based chains for CO₂ valorisation as added-value organic acids'—VIVALDI (ID: 101000441) from the Horizon 2020 Program of the European Commission; 2017-SGR-1462.

Availability of data and materials

The data that support the findings of this study are included in this article / supplementary files. Source data of figures and tables are available at figshare (<https://doi.org/10.6084/m9.figshare.25913494>).

Declarations

Ethics approval and consent to participate

Not applicable.

Consent for publication

Not applicable.

Competing interests

The authors declare no competing interests.

Received: 21 April 2024 Accepted: 20 June 2024

Published online: 15 July 2024

References

- Friedlingstein P, O'Sullivan M, Jones MW, Andrew RM, Bakker DCE, Hauck J, et al. Global carbon budget 2023. *Earth Syst Sci Data*. 2023;15:5301–69.
- Singh N, Ogunseitan OA, Wong MH, Tang Y. Sustainable materials alternative to petrochemical plastics pollution: a review analysis. *Sustain Horizons*. 2022;2.
- Singh A, Prajapati P, Vyas S, Gaur VK, Sindhu R, Binod P, et al. A comprehensive review of feedstocks as sustainable substrates for next-generation biofuels. *Bioenergy Res*. 2023;16:105–22. <https://doi.org/10.1007/s12155-022-10440-2>.
- Dürre P, Eikmanns BJ. C1-carbon sources for chemical and fuel production by microbial gas fermentation. *Curr Opin Biotechnol*. 2015;35:63–72.
- Love J. Microbial pathways for advanced biofuel production. *Biochem Soc Trans*. 2022;50:987–1001.
- Decker SR, Brunecky R, Yarbrough JM, Subramanian V. Perspectives on biorefineries in microbial production of fuels and chemicals. *Front Ind Microbiol*. 2023;1:11–11.
- Cho JS, Kim GB, Eun H, Moon CW, Lee SY. Designing microbial cell factories for the production of chemicals. *JACS Au*. 2022;2:1781–99.
- Becker J, Lange A, Fabarius J, Wittmann C. Top value platform chemicals: Bio-based production of organic acids. *Curr Opin Biotechnol*. 2015;36:168–75. <https://doi.org/10.1016/j.copbio.2015.08.022>.
- Gasparatos A, Stromberg P, Takeuchi K. Sustainability impacts of first-generation biofuels. *Anim Front*. 2013;3:12–26.
- Henning BG. The ethics of food, fuel & feed. *Daedalus*. 2015;144:90–8.
- Chilakamarry CR, Sakinah AMM, Zularisam AW, Pandey A. Glycerol waste to value added products and its potential applications. *Syst Microbiol Biomanufactur*. 2021;1:378–96. <https://doi.org/10.1007/s43393-021-00036-w>.
- Mujtaba M, Fernandes Fraceto L, Fazeli M, Mukherjee S, Savassa SM, Araujo de Medeiros G, et al. Lignocellulosic biomass from agricultural waste to the circular economy: a review with focus on biofuels, biocomposites and bioplastics. *J Clean Prod*. 2023;402, 136815.
- Niehoff PJ, Müller W, Pastoors J, Miebach K, Ernst P, Hemmerich J, et al. Development of an itaconic acid production process with Ustilaginaceae on alternative feedstocks. *BMC Biotechnol*. 2023;23:34.
- Baumschabl M, Ata Ö, Mattanovich D. Single carbon metabolism—a new paradigm for microbial bioprocesses? *Synth Syst Biotechnol*. 2024;9:322–9.
- Bachleitner S, Ata Ö, Mattanovich D. The potential of CO₂-based production cycles in biotechnology to fight the climate crisis. *Nat Commun*. 2023;14:6978.
- Lv X, Yu W, Zhang C, Ning P, Li J. C1-based biomanufacturing: advances, challenges and perspectives. *Bioresour Technol*. 2023;367:128259.
- Vásquez Castro E, Memari G, Ata Ö, Mattanovich D. Carbon efficient production of chemicals with yeasts. *Yeast*. 2023;40:583–93.
- Olivier A, Desgagnés A, Mercier E, Iliuta MC. New insights on catalytic valorization of carbon dioxide by conventional and intensified processes. *Ind Eng Chem Res*. 2023;62:5714–49.
- Statista. Production capacity of methanol worldwide from 2018 to 2022 [Internet]. GlobalData. 2024. <https://www.statista.com/statistics/1065891/global-methanol-production-capacity/#:~:text=The.global.production.capacity.of.million.metric.tons.in.2022>
- Sarwar A, Lee EY. Methanol-based biomanufacturing of fuels and chemicals using native and synthetic methylotrophs. *Synth Syst Biotechnol*. 2023;8:396–415. <https://doi.org/10.1016/j.synbio.2023.06.001>.
- Singh HB, Kang MK, Kwon M, Kim SW. Developing methylotrophic microbial platforms for a methanol-based bioindustry. *Front Bioeng Biotechnol*. 2022;10:1050740.
- Khlebodarova TM, Bogacheva NV, Zadorozhny AV, Bryanskaya AV, Vasilieva AR, Chesnokov DO, et al. *Komagataella phaffii* as a platform for heterologous expression of enzymes used for industry. *Microorganisms*. 2024;12:346.
- Barone GD, Emmerstorfer-Augustin A, Biundo A, Pisano I, Coccetti P, Mapelli V, et al. Industrial production of proteins with *Pichia pastoris*—*Komagataella phaffii*. *Biomolecules*. 2023;13:441.
- Wu X, Cai P, Gao L, Li Y, Yao L, Zhou YJ. Efficient bioproduction of 3-hydroxypropionic acid from methanol by a synthetic yeast cell factory. *ACS Sustain Chem Eng*. 2023;11:6445–53.
- Meesapyodsuk D, Chen Y, Ng SH, Chen J, Qiu X. Metabolic engineering of *Pichia pastoris* to produce ricinoleic acid, a hydroxy fatty acid of industrial importance. *J Lipid Res*. 2015;56:2102–9.
- Ávila-Cabré S, Pérez-Trujillo M, Albiol J, Ferrer P. Engineering the synthetic β-alanine pathway in *Komagataella phaffii* for conversion of methanol into 3-hydroxypropionic acid. *Microb Cell Fact*. 2023;22:237.
- Guo F, Dai Z, Peng W, Zhang S, Zhou J, Ma J, et al. Metabolic engineering of *Pichia pastoris* for malic acid production from methanol. *Biotechnol Bioeng*. 2021;118:357–71.
- Robert T, Friebe S. Itaconic acid—a versatile building block for renewable polyesters with enhanced functionality. *Green Chem*. 2016;18:2922–34.
- Devi N, Singh S, Manickam S, Cruz-Martins N, Kumar V, Verma R, et al. Itaconic acid and its applications for textile. *Pharma and Agro-Industrial Purposes Sustain*. 2022;14:13777.
- Willke T, Vorlop KD. Biotechnological production of itaconic acid. *Appl Microbiol Biotechnol*. 2001;56:289–95.
- Steiger MG, Blumhöff ML, Mattanovich D, Sauer M. Biochemistry of microbial itaconic acid production. *Front Microbiol*. 2013;4:23.
- Goldberg I, Rokem JS. Organic and fatty acid production, microbial defining statement introduction organic acids fatty acids conclusions further reading. In: Schaechter M, editor. *Encyclopedia of microbiology*, 3rd edn. Academic Press; 2009. pp. 421–442.
- Krull S, Hevekerl A, Kuenz A, Prüße U. Process development of itaconic acid production by a natural wild type strain of *Aspergillus terreus* to reach industrially relevant final titers. *Appl Microbiol Biotechnol*. 2017;101:4063–72.
- Bentley R, Thiessen CP. Biosynthesis of Itaconic Acid in *Aspergillus terreus*. *J Biol Chem*. 1957;226:703–20. [https://doi.org/10.1016/S0021-9258\(18\)70852-1](https://doi.org/10.1016/S0021-9258(18)70852-1).
- Dwiarti L, Yamane K, Yamatani H, Kahar P, Okabe M. Purification and characterization of cis-Aconitic acid decarboxylase from *Aspergillus terreus* TN484-M1. *J Biosci Bioeng*. 2002;94:29–33.
- Li A, van Luijk N, ter Beek M, Caspers M, Punt P, van der Werf M. A clone-based transcriptomics approach for the identification of genes relevant for itaconic acid production in *Aspergillus*. *Fungal Genet Biol*. 2011;48:602–11.
- Steiger MG, Punt PJ, Ram AFJ, Mattanovich D, Sauer M. Characterizing MttA as a mitochondrial cis-aconitic acid transporter by metabolic engineering. *Metab Eng*. 2016;35:95–104. <https://doi.org/10.1016/j.mben.2016.02.003>.
- Okabe M, Lies D, Kanamasa S, Park EY. Biotechnological production of itaconic acid and its biosynthesis in *Aspergillus terreus*. *Appl Microbiol Biotechnol*. 2009;84:597–606.

39. Klement T, Büchs J. Itaconic acid—a biotechnological process in change. *Bioresour Technol.* 2013;135:422–31. <https://doi.org/10.1016/j.biortech.2012.11.141>.
40. Teleyk BE, Vodnar DC. Recent advances in biotechnological itaconic acid production, and application for a sustainable approach. *Polymers (Basel).* 2021;13:3574.
41. Yang J, Xu H, Jiang J, Zhang N, Xie J, Wei M, et al. Production of itaconic acid through microbiological fermentation of inexpensive materials. *J Bioresour Bioprod.* 2019;4:135–42.
42. Prielhofer R, Barrero JJ, Steuer S, Gassler T, Zahrl R, Baumann K, et al. GoldenPICs: a golden gate-derived modular cloning system for applied synthetic biology in the yeast *Pichia pastoris*. *BMC Syst Biol.* 2017;11:123.
43. Gassler T, Heisteringer L, Mattanovich D, Gasser B, Prielhofer R. CRISPR/Cas9-mediated homology-directed genome editing in *Pichia pastoris*. *Methods Mol Biol.* 2019;1923:211–225.
44. Gasser B, Prielhofer R, Marx H, Maurer M, Nocon J, Steiger M, et al. *Pichia pastoris*: protein production host and model organism for biomedical research. *Future Microbiol.* 2013;8:191–208.
45. Kurtzman CP. Biotechnological strains of *Komagataella (Pichia) pastoris* are *Komagataella phaffii* as determined from multigene sequence analysis. *J Ind Microbiol Biotechnol.* 2009;36:1435–8.
46. Chang CH, Hsiung HA, Hong KL, Huang CT. Enhancing the efficiency of the *Pichia pastoris* AOX1 promoter via the synthetic positive feedback circuit of transcription factor Mxr1. *BMC Biotechnol.* 2018;18:81.
47. Hohenblum H, Borth N, Mattanovich D. Assessing viability and cell-associated product of recombinant protein producing *Pichia pastoris* with flow cytometry. *J Biotechnol.* 2003;102:281–90.
48. Pfaffl MW. A new mathematical model for relative quantification in real-time RT-PCR. *Nucleic Acids Res.* 2001;29:e45.
49. Baumschabl M, Ata Ö, Mitic BM, Lutz L, Gassler T, Troyer C, et al. Conversion of CO₂ into organic acids by engineered autotrophic yeast. *Proc Natl Acad Sci U S A.* 2022;119:e2211827119.
50. Zha J, Liu D, Ren J, Liu Z, Wu X. Advances in metabolic engineering of *Pichia pastoris* strains as powerful cell factories. *J Fungi.* 2023;9:1027.
51. Soares-Silva I, Ribas D, Sousa-Silva M, Azevedo-Silva J, Rendulic T, Casal M. Membrane transporters in the bioproduction of organic acids: State of the art and future perspectives for industrial applications. *FEMS Microbiol Lett.* 2020;367:fnaa118.
52. Totaro D, Radoman B, Schmelzer B, Rothbauer M, Steiger MG, Mayr T, et al. Microscale perfusion-based cultivation for *Pichia pastoris* clone screening enables accelerated and optimized recombinant protein production processes. *Biotechnol J.* 2021;16:e2000215.
53. Çalik P, Ata Ö, Güneş H, Massahi A, Boy E, Keskin A, et al. Recombinant protein production in *Pichia pastoris* under glyceraldehyde-3-phosphate dehydrogenase promoter: from carbon source metabolism to bioreactor operation parameters. *Biochem Eng J.* 2015;95:20–36.
54. Wang Y, Guo Y, Cao W, Liu H. Synergistic effects on itaconic acid production in engineered *Aspergillus niger* expressing the two distinct biosynthesis clusters from *Aspergillus terreus* and *Ustilago maydis*. *Microb Cell Fact.* 2022;21:158.
55. Kim J, Seo HM, Bhatia K, Song HS, Kim JH, Jeon JM, et al. Production of itaconate by whole-cell bioconversion of citrate mediated by expression of multiple cis-aconitate decarboxylase (*cadA*) genes in *Escherichia coli*. *Sci Rep.* 2017;7:39768. <https://doi.org/10.1038/srep39768>.
56. Lian J, Si T, Nair NU, Zhao H. Design and construction of acetyl-CoA overproducing *Saccharomyces cerevisiae* strains. *Food, Pharm Bioeng Div 2014 - Core Program Area 2014 AIChE Annu Meet 2014*;2:750–60. <https://doi.org/10.1016/j.jymben.2014.05.010>.
57. Liew FE, Nogle R, Abdalla T, Rasor BJ, Canter C, Jensen RO, et al. Carbon-negative production of acetone and isopropanol by gas fermentation at industrial pilot scale. *Nat Biotechnol.* 2022;40:335–44.
58. Gopaliya D, Kumar V, Khare S. Recent advances in itaconic acid production from microbial cell factories. *Biocatal Agric Biotechnol.* 2021;36:102130.
59. Becker J, Tehrani HH, Ernst P, Blank LM, Wierckx N. An optimized *Ustilago maydis* for itaconic acid production at maximal theoretical yield. *J Fungi.* 2020;7:20.
60. Lim CK, Villada JC, Chalifour A, Duran MF, Lu H, Lee PKH. Designing and engineering *Methylorubrum extorquens* am1 for itaconic acid production. *Front Microbiol.* 2019;10:1027.
61. Chin T, Sano M, Takahashi T, Ohara H, Aso Y. Photosynthetic production of itaconic acid in *Synechocystis* sp. PCC6803. *J Biotechnol.* 2015;195:43–5.
62. Li A, Pfelzer N, Zuijderwijk R, Brickwedde A, Van Zeijl C, Punt P. Reduced by-product formation and modified oxygen availability improve itaconic acid production in *Aspergillus niger*. *Appl Microbiol Biotechnol.* 2013;97:3901–11.
63. van der Straat L, Vernooij M, Lammers M, van den Berg W, Schonewille T, Cordewener J, et al. Expression of the *Aspergillus terreus* itaconic acid biosynthesis cluster in *Aspergillus niger*. *Microb Cell Fact.* 2014;13:11.
64. Wierckx N, Agrimi G, Lübeck PS, Steiger MG, Mira NP, Punt PJ. Metabolic specialization in itaconic acid production: a tale of two fungi. *Curr Opin Biotechnol.* 2020;62:153–9.
65. Li QZ, Jiang XL, Feng X-J, Wang JM, Sun C, Zhang H-B, et al. Recovery processes of organic acids from fermentation broths in the biomass-based industry. *J Microbiol Biotechnol.* 2016;26:1–8.
66. Kanamasa S, Dwiarti L, Okabe M, Park EY. Cloning and functional characterization of the cis-aconitic acid decarboxylase (CAD) gene from *Aspergillus terreus*. *Appl Microbiol Biotechnol.* 2008;80:223–9.

Publisher's Note

Springer Nature remains neutral with regard to jurisdictional claims in published maps and institutional affiliations.